

Betatron Scraping at RHIC: General Remarks and Sample Calculations

A. J. Stevens

September 1992

Collider Accelerator Department
Brookhaven National Laboratory

U.S. Department of Energy

USDOE Office of Science (SC)

Notice: This technical note has been authored by employees of Brookhaven Science Associates, LLC under Contract No. DE-AC02-76CH00016 with the U.S. Department of Energy. The publisher by accepting the technical note for publication acknowledges that the United States Government retains a non-exclusive, paid-up, irrevocable, world-wide license to publish or reproduce the published form of this technical note, or allow others to do so, for United States Government purposes.

DISCLAIMER

This report was prepared as an account of work sponsored by an agency of the United States Government. Neither the United States Government nor any agency thereof, nor any of their employees, nor any of their contractors, subcontractors, or their employees, makes any warranty, express or implied, or assumes any legal liability or responsibility for the accuracy, completeness, or any third party's use or the results of such use of any information, apparatus, product, or process disclosed, or represents that its use would not infringe privately owned rights. Reference herein to any specific commercial product, process, or service by trade name, trademark, manufacturer, or otherwise, does not necessarily constitute or imply its endorsement, recommendation, or favoring by the United States Government or any agency thereof or its contractors or subcontractors. The views and opinions of authors expressed herein do not necessarily state or reflect those of the United States Government or any agency thereof.

AD/RHIC/RD-45

RHIC PROJECT

Brookhaven National Laboratory

Betatron Scraping at RHIC: General Remarks and Sample Calculations

A. Stevens

September 1992

Betatron Scraping at RHIC: General Remarks and Sample Calculations

A. Stevens

I. Introduction

A betatron scraper is a physical aperture whose primary purpose is to intercept particle trajectories whose amplitude is outside the dynamic aperture. Such "halo" trajectories can arise, for example, from the "tail" of beam-beam or beam-gas elastic scattering. In the absence of such a scraper in RHIC, trajectories outside the dynamic aperture would likely encounter either the internal dump or the vacuum pipe at a maximum beta quadrupole. The internal dump would be expected, for reasons discussed in section II below, to be very inefficient as a beam scraper, which means that stray ions would be likely to barely "clip" either one end or the other of the dump aperture and interact elsewhere in the lattice. In any event, therefore, the absence of a strategically placed beam scraper implies a reasonably high probability that stray ions will interact near maximum beta locations and cause undesirable backgrounds in detectors.

A "secondary" purpose of a betatron scraper is deliberate beam scraping to shave away a part of the transverse beam tails. This function may be important for beam studies or for experiments, such as a pp elastic scattering measurement¹, which may be particularly sensitive to such tails. Although efficient scraping is less critical in this mode, where experiments are presumably "turned off" during the scraping process, it is still desirable in order to restrict the radiation from the shaving process to as few locations as possible. This note does not consider deliberate tail-shaving in detail, but some calculations related to limitations on the beam shaving rate are presented in section V below.

In the next section attention is given to general considerations which dictate the optimal choice for many of the characteristics of an efficient betatron scraper. Sections III and IV describe simulations of the scraping process which are based on measurements of betatron amplitude growth at the CERN SPS.² These simulations are not intended to represent the situation which will exist at RHIC, but are presented as "sample calculations" whose purpose is illustrative rather than definitive.

II. General Considerations

The first general consideration is a qualitative discussion of the length and tilt (relative to the beam direction) of a beam scraper which is shown schematically in Fig. 1.

The scraping efficiency, defined as the fraction of incident beam particles which interact in the scraper, is maximum for orbits which are parallel to the front edge as shown. Orbits which have a significant slope with respect to the edge will in general "clip" either the front or back edge as also illustrated in Fig. 1; their orbits and energy will be slightly perturbed and they may interact elsewhere in the lattice before again returning to the scraper position with an appropriate phase. This condition of parallelism can be met for on-momentum particles at a single point in the lattice, say the front edge of the scraper, by aligning the scraper with a tilt of $-\alpha \cdot X/\beta$ where α and β are the usual lattice functions at this point and X is the displacement of the front edge from the beam axis in the coordinate of scraping (discussed below). Two conclusions follow from this consideration: (1) since, strictly speaking, parallelism can be obtained only at a single point, the scraper should in principle be as short as possible, i.e., only a "few" interaction lengths, and (2) since RHIC is designed to operate with widely varying lattice functions in the intersection regions, the scraper must have an adjustable position and tilt. Neither of these characteristics of an efficient scraper are met by the internal dump.

Secondly, we consider the transverse coordinate(s) and lattice location(s) of the scraper(s). It is by no means obvious that efficient scraping in both the horizontal and vertical coordinates is required: both experience at FNAL³ and simulations of RHIC³ indicate that horizontal, vertical coupling transform disturbances in one transverse coordinate to the other within a few hundred orbits. We will therefore assume that scraping in only one coordinate is necessary and take that to be the horizontal (bending plane, called "X") coordinate adopting the philosophy that "more is going on" in this plane.⁵ Ideally, the scraper position within an intersection region should be: (a) a large distance upstream of any superconducting magnet, (b) downstream of the crossing point, and (c) at a position with large β value in the X coordinate. The last of these attributes again follows from the desire to maximize the efficiency of the scraper. The absorption probability for parallel halo particles incident on the front edge of the scraper increases with the displacement $-\delta X$ in Fig. 1. This displacement, in turn, is proportional to the square root of the β function times the change (over some number of orbits) of the particle's amplitude. All these conditions are met in the RHIC 92 lattice immediately downstream of Q3 (Inner Arc) at the 4, 8, and 12 o'clock intersection regions.

Some information on the choice of material for the scraper likewise follows from the desire to optimize the scraping efficiency in the approximation that inefficiency is dominated by small angle multiple scattering. Particles entering parallel to the scraper at a fixed value of δX obtain, after traversing a distance L , a Gaussian distribution in X whose rms width is $L \cdot \theta_{rms}$. Since θ_{rms} goes as the square root of L/L_{rad} , the best choice of material (from this consideration only) would be the material which minimizes $L^{3/2}/L_{rad}^{1/2}$ evaluated at $L = L_{abs}$. This quantity has been evaluated for Al, Fe, and W with the result that Fe (steel) appears to be the optimal choice.⁶

The last general consideration examines the question of how many betatron scrapers per ring are required. It was pointed out above that a single scraper cannot be optimized

for both horizontal and vertical coordinates and we have already assumed, barring evidence to the contrary from operational experience, that optimal scraping in the vertical coordinate is not essential. Similarly, a single scraper cannot be absolutely optimized for both heavy ions and protons because of the different values of the absorption lengths. Finally, the possibility of "secondary scrapers" must be considered. These are adjustable apertures intended to intercept some fraction of halo particles which escape (outscatter) from the primary scraper. Both the effect of scraper length and the performance of a secondary scraper are simulated in one of the "sample calculations" described below.

III. Betatron Growth Assumptions and Simulation Codes

To estimate the efficiency of the scraping process a model for the amplitude growth of beam halo particles is required. For this purpose we rely on the halo growth measurements at the SPS described in Ref. 1. Briefly, these measurements proceeded as follows. A scraper was inserted in the beam halo to some transverse lateral distance X_1 , then rapidly withdrawn a distance ΔX . After some time Δt , the background from halo particles striking the scraper begins to rise rapidly, so that the average velocity (in the interval between X_1 and $X_1 + \Delta X$) is $\Delta X/\Delta t$. Measuring this quantity as a function of X_1 gives the X dependence of this quantity. The results are reasonably well represented by the following expression:

$$v_t = 2.45 \cdot (e^{(X-4)/1.8} - 1)$$

where X is measured in units of σ (rms beam size) and v_t is the average transverse velocity in σ per second. In this approximation of the results of Ref. 1, the halo growth is zero at 4σ (the "dynamic aperture"), is $5\sigma/\text{sec}$ at $X=6\sigma$, and increases to $37\sigma/\text{sec}$ at $X=9\sigma$. The reason for this exponential halo growth is attributed to increasing non-linear magnetic field components as the particles approach the magnet apertures.

There is no reason to suppose that the magnetic imperfections in the RHIC lattice will closely resemble those at the SPS or that the measured beam size in a "real" machine is precisely the same as a theoretical beam size. Nevertheless, in the absence of a real machine, scraping simulations based on the SPS measurement may be as well as one can do and should at least provide useful qualitative information on the efficiency of the scraping process. The assumption that all accelerators are like the SPS (in this regard) is also being made for scraping simulations for the CERN LHC.⁷

The simulations proceeded in two steps. In the first step, a Monte Carlo computer program was written to simulate halo growth from some point outside the "dynamic aperture" (whose value depends on differing assumptions described in the next section) to the (varied) transverse position of the scraper. In this program orbits at the front edge of the scraper are assumed to be represented by $X(t) = a(t) \cdot \sqrt{\beta} \cdot \cos(\psi) + X_p \cdot \Delta P/P$ where β

and X_p are the beta function and dispersion at this point which is 1m downstream of Q3 in the inner arc (see section II above) and $a(t)$ describes the growing amplitude in units of the square root of the emittance.⁸ The program tracks particles one revolution at a time until they are incident on either the front edge or face of the scraper. In all cases $\Delta P/P$ is sampled uniformly in the interval $\pm 0.2\%$ and the machine tune is taken as 28.826. The output of this program is a file of positions on the scraper (X,Z) and directions (dX/dZ).

The second step of the simulation is transport of the particles through the scraper which is accomplished by the computer code ELSHIM.⁹ This code is a modification (to include heavy ions) of the program ELSIM¹⁰ which is used at FNAL, CERN, and elsewhere for transport of protons in geometries where the presence of edges are important. ELSHIM tracks particles (ions or protons) until either they escape the scraper or are "absorbed", where "absorption" includes both nuclear absorption and processes which cause the particle to lose more than 5% of its initial energy. The scraping efficiency is defined as the ratio of absorbed particles to incident particles. The current version of ELSHIM does not simulate in detail processes which may change Z or A by one or two units (e.g. - electron capture), so that ions which escape are assumed to have the incident Z and A values.

IV. Sample Calculations

The first exercise performed, whose primary purpose was to estimate the scraping efficiency for Au ions compared to protons and the sensitivity of efficiency to both length and tilt angle of the scraper, was essentially a "literal" interpretation of the SPS measurement. In this simulation the dynamic aperture was assumed to be at 4σ and the front edge of the scraper at 6σ with the conventional CDR definition of sigma at 10π invariant emittance, i.e., $\sigma^2(\text{amplitude}) = 10 \times 10^{-6} / (6 \cdot \beta \gamma)$. For this case the change in particle amplitude per revolution was assumed to be $\delta a = 2.45 \cdot \sigma \cdot \Delta t \cdot (e^{(a/\sigma-4)/1.8} - 1)$ where $\Delta t = 12.6 \mu\text{sec}$. The lattice functions were taken as those appropriate for β^* (beta at the crossing point) = 6m in the RHIC92 lattice.¹¹ Computer runs were made for scraper lengths of 10 and 30 cm. for Au ions and 30 cm. for protons, and 500 halo particles per tilt angle were generated and followed.

Fig. 2 shows the lateral displacement (δX in Fig. 1) on the front edge of the 10 cm. scraper for Au ions at the optimal tilt value ($-\alpha \cdot X/\beta$). The mean of this distribution depends, as discussed in section II, on the β function at the scraper edge and the spread is primarily due to phase variations after the halo particles have achieved sufficient amplitude to intercept the scraper. The result of this simulation is shown in Fig. 3. The sensitivity to scraper length is seen to be small, at least in the range explored. At the optimal tilt, scraping inefficiency of $\sim 12\%$ for the Au ions which is ~ 4 -5 times better than that for protons. This quantifies the qualitative expectation that Au scraping should be "much better" than protons because of the shorter absorption length and the smaller (by Z/A) rms

scattering angle. The sign of the relative tilt angle in Fig. 3 is such that positive angles correspond to the downstream end of the scraper being further away from the beam axis. The asymmetry in the tilt angle sensitivity is due to the fact that the negative tilt has a scraper end at a smaller distance from the beam axis than the positive tilt and, at this smaller distance, the halo amplitude is growing more slowly. We conclude from Fig. 3 that the scraper tilt angle should be aligned to within $\sim 25 \mu\text{rad}$. for efficient betatron scraping.

This exercise was also used to estimate the efficacy of a secondary scraper. A linear tracking program was written to follow Au orbits which escape¹² the scraper from the point of escape to the relatively long drift region (13.7m) between Q7 and Q8 which was considered a reasonable candidate for the location of such a scraper. A position 6m downstream of Q7 represents a (somewhat arbitrary) compromise between the phase advance between the scraper and this position, 117.5° for $\beta^* = 6\text{m}$, and allowing significant space to the next superconducting magnet (Q8).¹³ The 49 (of 500) Au ions which escape the "primary" 10 cm. scraper in the optimal tilt run were tracked to this position where an aperture at $10\sigma + 1\text{ mm}$. (7.5 mm for the β value at this position) is assumed to exist on the opposite side of the beam center line from the primary scraper. Of these 49, 20 outscattered trajectories have an $|X|$ value $> 4\text{ cm}$. at the first aperture check at Q4, and 2 more exceed this value between Q4 and Q7 which leaves 27 trajectories within the physical aperture at the position of the secondary scraper. If the primary scraper is on the ring-inside of the beam center line and the secondary scraper on the ring-outside, only 3 of these 27 trajectories intercept the secondary scraper whereas if these positions are reversed, 23 of the 27 encounter the secondary scraper. This asymmetry is easily understood as the consequence of energy loss in the primary scraper: since the two bending magnets in this section of the insertion region, B5I and BSI, bend positives toward ring center, the deflection from both phase advance and dispersion have the same sign in the latter configuration.

The purpose of the second exercise performed was to simulate scraping efficiency as a function of insertion region tune which is conveniently characterized by the value of β^* . In this exercise, the scraper was positioned 2 mm. inside the "shadow" of the internal dump and a dynamic aperture assumed inside this physical aperture. In terms of particle amplitude, the dynamic aperture, a_{dy} (in $\downarrow\text{m}$) is assumed to be:

$$a_{dy} = 0.72 \cdot \downarrow \beta^* \cdot 10^{-3}$$

This value is roughly in agreement with tracking studies which have been performed in the RHIC92 lattice.¹⁴ In the same units, the dump aperture¹⁵, a_{dp} , and scraper aperture, a_s , are given by:

$$a_{dp} = .014 / \downarrow \beta_d \text{ where } \beta_d = \max(\beta_H, \beta_v) \text{ at the dump}$$

and

$$a_s = (a_{dp} \cdot \downarrow \beta_s - .002) / \downarrow \beta_s \text{ where } \beta_s = \beta_H \text{ at the scraper}$$

The following table results:

Table I. β values and assumed apertures in the second scraping simulation

β^* (m)	a_{dy} (\downarrow mX10 ⁻³)	β_d (m)	a_{dp} (\downarrow mX10 ⁻³)	β_s (m)	a_s (\downarrow mX10 ⁻³)
10	2.277	25.2	2.789	142.1	2.621
6	1.764	39.8	2.219	220.7	2.084
2	1.018	89.0	1.484	635.8	1.405
1	0.720	152.2	1.135	1256.4	1.078

As in the previous exercise, it is necessary to model the amplitude growth for particles whose amplitude exceeds a_{dy} . In this case we take the growth in amplitude per revolution to be $\delta a = 0.5 \times 10^{-3} \cdot \Delta t \cdot (\exp(a/a_{dy})/0.45 \cdot a_{dy} - 1)$. In this expression the exponential rise relative to a_{dy} is the same as taken previously and the coefficient is approximately $2.45 \cdot \sigma$ where " σ " is the average of the theoretical beam sizes at 10π and 60π invariant emittance.

The efficiency as a function of β^* for Au ions at the optimal tilt for a 10 cm. scraper is shown in Fig. 4. The increase in efficiency as β^* decreases is due to both to the higher value of β_s and a larger exponential growth factor at the smaller β^* values. The latter factor is, of course, a consequence of the formula assumed for the dynamic aperture and may well not be indicative of the actual situation at RHIC. It is interesting to note that the amplitude growth, δa per revolution at $a=a_s$, at $\beta^* = 6$ m is a factor of 6 smaller than the corresponding amplitude growth in the first exercise. The fact that the efficiency is 90%¹⁶ in both cases encourages belief that the sample calculations performed here are not overly sensitive to the models assumed.

V. Limitations on Beam Shaving

The amount of beam interacting on a betatron scraper during normal running has been estimated¹⁷ to be of the order of 10% of the initially stored beam over the 4-10 hours of a physics run. This slow loss rate is of little concern for either the scraper itself or the superconducting magnets downstream of the scraper, the nearest of which has been assumed here to be Q4. However, as mentioned in the introduction, deliberately shaving the beam by moving the scraper into the tail may be desirable on occasions. In this case two concerns arise: (1) the possibility of quenching Q4, and (2) the possibility of damaging the scraper itself from overheating.

Energy deposition in Q4 has been estimated by utilizing the hadron cascade program CASIM¹⁸ in the geometry shown in Fig. 5. Au ions at 100 GeV/u, chosen randomly over the first 10 microns laterally and the first 10 cm. in the beam direction, are forced to

interact in the 30 cm. long steel "scraping wedge" shown which is displaced by 2.5 cm. from the beam axis.¹⁹ Energy deposition was calculated in the coil region of Q4 which extends radially from 4 cm. to 5 cm. and is 1.85m long. The material of the coil is approximated by reduced density ($\rho = 6 \text{ g/cm}^3$) Fe. The magnetic field was assumed to the $\beta^* = 6\text{m}$ design value¹¹ within the aperture and ignored in the coil and yoke regions. The coil was divided into 6 regions in Z, 2 in R, and 4 in the azimuthal coordinate to study the spacial variation of energy deposition density. The dashed "collar" shown in Fig. 5 immediately in front of Q4 is a 2m long steel cylinder which begins radially at $R = 3.15 \text{ cm}$. Computer runs were made with and without this protective collar to determine its effect.

The energy deposition density in the inner radial region of the coil was found to be $\sim 40\%$ higher than in the outer. In both unprotected and protected geometries, the location of maximum energy density was at the downstream end of Q4 on the opposite side of the beam axis from the scraping wedge. In the inner radial region these energy densities are $25.1 \pm 4.5 \times 10^{-3} \text{ GeV/cm}^3 \cdot \text{ion}$ (unprotected) and $9.9 \pm 1.9 \times 10^{-3} \text{ GeV/cm}^3 \cdot \text{ion}$ (protected). The number of ions that can be shaved without quenching Q4 can be determined from these energy densities together with the experimentally determined FNAL quench thresholds of $\sim 2 \text{ mJ/g}$ for instantaneous loss²⁰ or $\sim 8 \text{ mW/g}$ for beam loss over times in the 1-10 second range.²¹ The unprotected energy density of $25.1 \text{ GeV/cm}^3 \cdot \text{ion}$ gives upper limits of $\sim 3 \times 10^9$ ions, or 5.3% of the design intensity of 5.7×10^{10} ions, for instantaneous shaving, and 21% of the design intensity per second for shaving over times of the order of seconds. Since tail shaving should involve no more than a few per cent of the beam and can (or **must** as discussed below) take place over several seconds, the CASIM calculations indicate that no protection of Q4 is required.

Of much greater concern when considering deliberate shaving of heavy ions is the integrity of the scraper itself. The problem is the very high dE/dx ionization energy loss of heavy ions in the small volume represented by the front of the scraper edge. This note confines itself to rough arguments intended to estimate the order of magnitude of the time scale over which 1% of the Au beam can be shaved. First, we assume that the scraper can be moved into the tail of the beam at the same rate (typically several mm/sec) as the halo growth rate assumed in section III above. If this is the case, then a δx distribution on the scraper edge similar to that shown in Fig. 2 can be achieved. We simplify that distribution in this discussion by assuming a flat δx width of 15 microns ($15 \times 10^{-4} \text{ cm}$). Some portion of the beam tail is then incident on the front face of the scraper over an area $\delta A = \delta x \cdot \delta y$ where δy is determined by the vertical beam size. In the RHIC92 lattice, the vertical β function at the scraper for the $\beta^* = 6\text{m}$ tune is approximately 83m. The 1σ vertical beam size at 10π emittance is 1.13 mm which gives a δA containing 68% of the tail portion under consideration equal to $3.4 \times 10^{-4} \text{ cm}^2$. If we denote the number of Au ions to be shaved by N_b , then the energy density from dE/dx at the front edge of the scraper is given by:

$$\delta E(\text{GeV/g}) = N_b \times (.68/\delta A) \times (79)^2 \times 1.6 \times 10^{-3} \text{ GeV/g/cm}^2$$

The next step in the argument is to determine the value of N_b which can be shaved

instantaneously, i.e., with no heat transfer out of the small volume of the scraper being considered. We will assume that an instantaneous temperature rise which induces a tensile stress equal to 50% of the steel strength is allowable. This corresponds, in the context of a conservative model as discussed elsewhere,²² to approximately 198 °C. Given this limit and the specific heat of 0.110 cal/g°C of AISI 430 steel, N_b is determined from the formula above to be 2.85×10^7 Au ions which is 0.05% of the full beam intensity and 5% of the assumed goal of the shaving.

We now estimate the time required for the heat in the scraper edge to dissipate so that another 0.05% of the beam can be shaved. The mass of the scraper itself provides a "heat sink" for this dissipation, but, because steel has a poor thermal conductivity, another material such as copper²³ is preferable. The thermal mass required is not large; If 10% of the energy of the 1% of the beam to be shaved ends up in the scraper, a 1 °C temperature rise requires only 467 grams of copper.²⁴ We will assume in this exercise, therefore, that the scraper consists of a 1mm thick steel "face" mounted on a copper block. In the approximation that the copper thermal conductivity is infinite, the heat dissipation calculation is reduced to determining the time required for a 15 micron thick region of steel which has been heated to 198 °C above ambient (which we take to be 22 °C) to cool to near-ambient by heat conduction across a 1 mm steel layer to a boundary which is held at the ambient temperature by the thermal mass of the copper. Fig. 6 illustrates the computation which was performed by utilizing the computer program HEATING5.²⁵ As shown in this figure, an initial ($t = 0$) temperature of 220 °C is assumed in a steel region extending to 15μ which decreases linearly to 22 °C at 1 mm. At some later time, the hot region is ΔT above ambient. With a constant thermal conductivity for steel of 0.163 J/sec•cm•°C, ΔT is reduced to 1 °C in 600 msec. The time to required to scrape 1% of the Au beam is therefore nominally 12 sec. We emphasize that this conclusion is based on the critical assumption that the scraper motion can achieve an effective beam width of 15 microns on the scraper edge.

Although a more sophisticated study of this problem should be undertaken, it would seem likely that maintaining the scraper's integrity is the limiting factor in deliberate heavy ion beam shaving and that a "smart scraper", capable of stopping its motion when a certain level of radiation is detected, will be required.

VI. Summary/Recommendation

We have examined general considerations which define the characteristics of an optimized betatron beam scraper and performed simulations to estimate the sensitivity of halo scraping efficiency to some of those characteristics. These model-dependent simulations, though not definitive, suggest the following: (1) that a single steel-faced scraper can obtain $\sim 90\%$ scraping efficiency for Au ions in contrast to $\sim 50\%$ for protons, (2) that the scraping efficiency for heavy ions is relatively insensitive to modest departures from the

optimum scraper length, and (3) that an angular alignment of $\sim 25 \mu\text{rad}$ is required to maintain high scraping efficiency.

Limitations on deliberate beam shaving, whose time scale is seconds in contrast to the hours over which halo growth is assumed to occur, have also been examined. The most severe potential problem on this time scale is the possibility of damaging the scraper by overheating if heavy ions are shaved too rapidly. A rough calculation indicates that the time for shaving 1% of the design Au beam intensity must be greater than ~ 10 seconds.

Based on both the general considerations and simulations, we suggest that a reasonable day-1 scenario would be to deploy a single 20-30 cm. long L-shaped steel-faced scraper immediately downstream of the Q3I magnets in each ring at the 12 o'clock insertion region. Such a scraper would allow efficient horizontal scraping of heavy ions and less efficient vertical and/or proton beam scraping if required. Although the halo scraping simulation performed here suggests that "secondary scrapers" may be effective for heavy ions, we suggest that their deployment be deferred until mandated by operational experience. The 12 o'clock location is preferred since the scraper may well be a significant source of radiation¹⁷ and this location is far away from both the Collider Center and the site boundary.

References/Footnotes

1. W. Guryn et. al., RHIC Letter of Intent #1.
2. L. Burnod and J.B. Jeanneret, "Transverse Drift Speed Measurement of the Halo in a Hadron Collider", Proceedings of the Workshop on Advanced Beam Instrumentation, KEK, p. 375 (1991).
3. M. Harrison, private communication.
4. G. Parzen, private communication.
5. Both vertical and horizontal scraping can be done with the same scraper by making it "L"-shaped and adjustable in both planes. This is, in fact, the shape of the scraper at FNAL.² However, as discussed in the text, the coordinate with larger β is expected to be more efficient than the other.
6. This result follows from the expressions: $L_{\text{rad}} (\text{cm}) \sim A/\{\rho \cdot Z \cdot (Z+1) \cdot \ln[183/Z^{1/3}]\}$ and $L_{\text{abs}} (\text{cm}) \sim A/\{\rho \cdot [A_{\text{inc}}^{1/3} + A^{1/3}]^2\}$ where Z , A and ρ characterize the material. For $A_{\text{inc}} = 197$ (Au), Fe and Al are the best, but Al is less desirable from the length consideration. For protons, Al is much worse than Fe or W, which are approximately equal.

7. L. Burnod, private communication.
8. The time dependence of the amplitude follows from the parameterization of the SPS measurement given in the text and the assumption that $v_t = dX(\max)/dt = \sqrt{\beta} \cdot da/dt$.
9. A. Van Ginnekin, "ELSHIM; Program to Simulate Elastic Processes of Heavy Ions," BNL-47618, AD/RHIC-109 (1992).
10. A. Van Ginneken, "Elastic Scattering in Thick Targets and Edge Scattering," Phys. Rev. D, Vol. 37, p. 3292 (1988).
11. Lattice parameters are courtesy of S. Tepikian
12. Recall that the Z and A values of the escaped orbits are assumed to have the initial (incident) values.
13. The optimal phase advance depends on the average phase change in the scraper and may well be different for protons and heavy ions. For protons, a value near 160° is considered optimal.²
14. G.F. Dell, private communication. This value is approximately the **minimum** aperture in an ensemble of 10 random "machines" with differing arrangements of multipole field errors. [Subsequent to the calculations described here, a calculation reported by G. Parzen, AD/RHIC/AP-104, gives somewhat larger dynamic apertures at the high values of β^* than assumed here.]
15. The internal dump is assumed to have a physical aperture of 1.4 cm.
16. The exact agreement is fortuitous. Both values have a $1-\sigma$ statistical error of 1.3%
17. M. Harrison and A.J. Stevens, "Beam Loss Scenario in RHIC," RHIC Technical Note in preparation; draft version 6 dated 04/01/92.
18. A. Van Ginneken, "CASIM; Program to Simulate Hadron Cascades in Bulk Matter," Fermilab FN-272 (1975). A.J. Stevens, "Improvements in CASIM; Comparison with Data," AGS/AD/Tech. Note No. 296 (1988). See also A.J. Stevens, "Maximum Energy Deposition in the Internal Dump," AD/RHIC/RD-41 (1992). The last reference describes changes to CASIM to propagate fragments resulting from heavy ion collisions.
19. As discussed in section IV, some Au ions outscatter from the face of the scraper and intercept the vacuum pipe between the scraper and Q4. The contribution of these particles to the energy deposition in Q4 was examined in a separate series of computer runs and was found to be negligible at the level (20 of 500 [4%] incident ions) determined in section IV for optimal scraping. This source is not significant below the 30% level.

20. R. Dixon, N.V. Mokhov, and A. Van Ginneken, "Beam Induced Quench Study of Tevatron Dipoles," Fermilab FN-327 (1980).
21. F. T. Cole et. al., Eds., "Report on the Design of the FNAL Superconducting Accelerator," Batavia (1979).
22. A.J. Stevens, "Maximum Energy Deposition Densities in the Internal Dump," AD/RHIC/RD-41 (1992). See especially section VI of this reference which discusses the conservative model used for stress evaluation.
23. Unfortunately, the scraper cannot be made entirely of copper because of the strict flatness requirement for efficient scraping.
24. The specific heat of copper is taken to be $0.092 \text{ cal/g}^\circ\text{C}$
25. W.D. Turner, et. al., "HEATING5 - An IBM 360 Heat Conduction program," ORNL/CSD/TM-15 (1977).

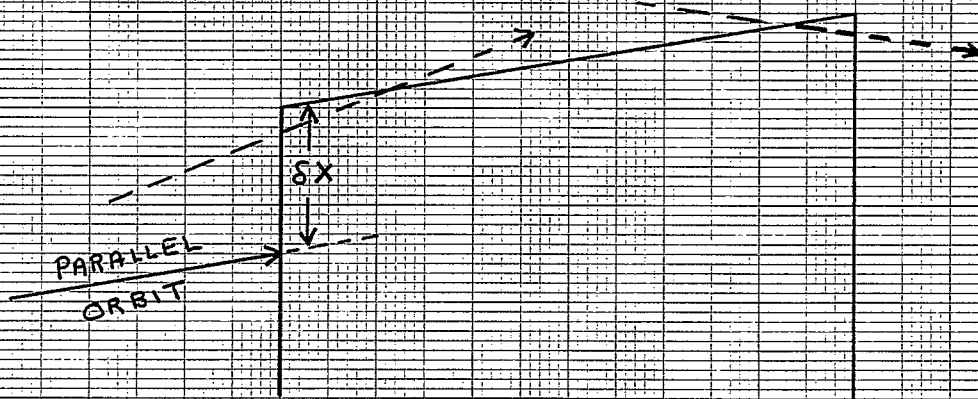


Fig 1 Schematic Illustration of Trajectories
Intercepting Scraper Block

Events/micron

30

20

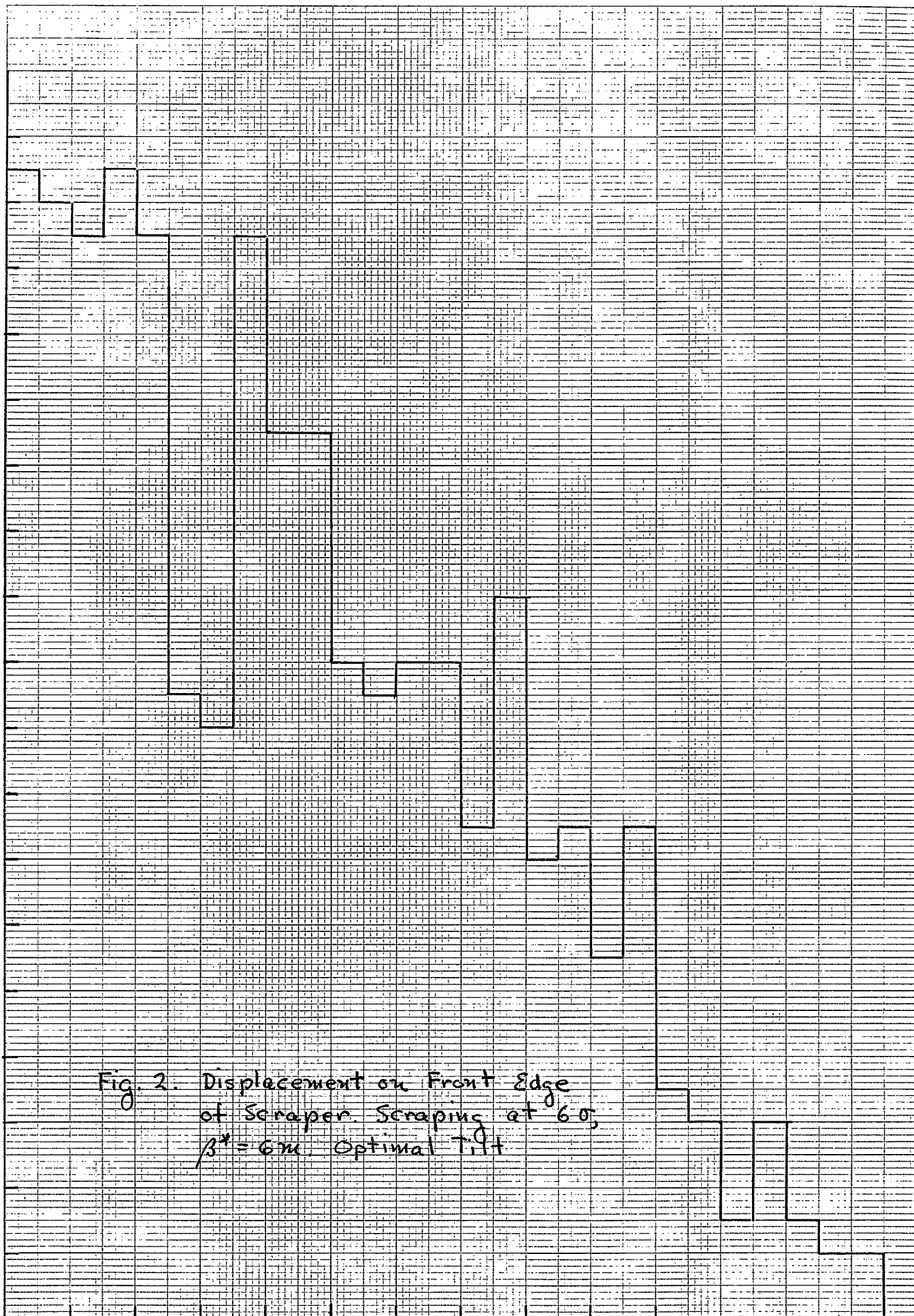
10

Fig. 2. Displacement on Front Edge
of Scraper. Scraping at 60;
 $\beta^* = 6m$. Optimal Tilt

10

δx in microns

20



Scraping Efficiency (%)

90
80
70
60
50
40
30
20
10

- Au at 100 GeV/u, L = 10 cm.
- Au at 100 GeV/u, L = 30 cm.
- Protons at 100 GeV, L = 30 cm.

Fig. 3 Scraping Efficiency vs. Scraper Tilt
Relative to optimal Tilt. Scraping
at 60°, $\beta^* = 6$ m.

-50

0

+50

+100

Relative Scraper Tilt (μ rad.)

46 1320

K&E 10 X 10 TO 1/2 INCH 7 X 10 INCHES
KEUFFEL & ESSER CO. MADE IN U.S.A.

Scraping Efficiency (%)

90

80

70

60

50

40

30

20

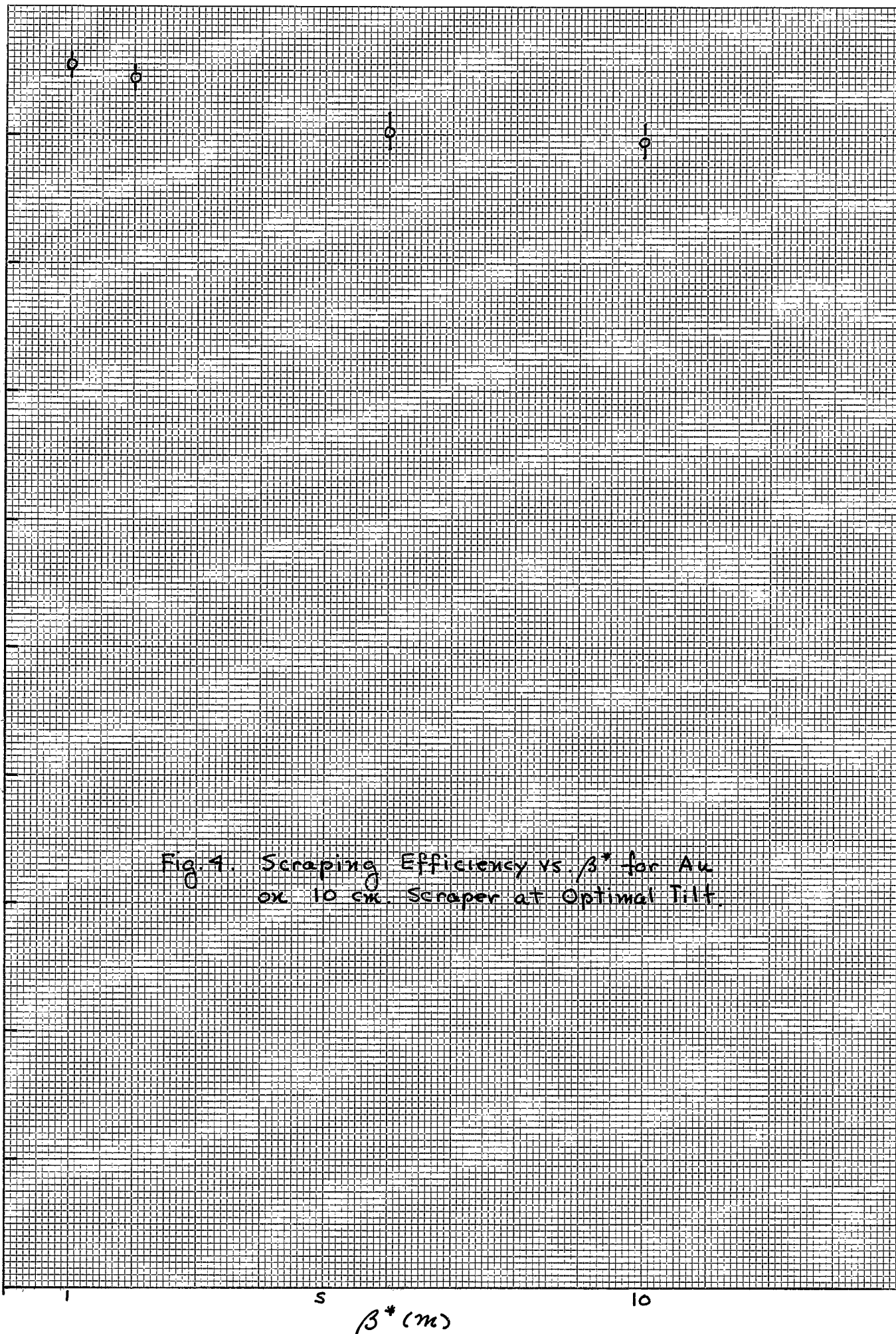
10

S

10

 $\beta^* (m)$

Fig. 4. Scraping Efficiency vs. β^* for Au
on 10 cm. Scraper at Optimal Tilt.



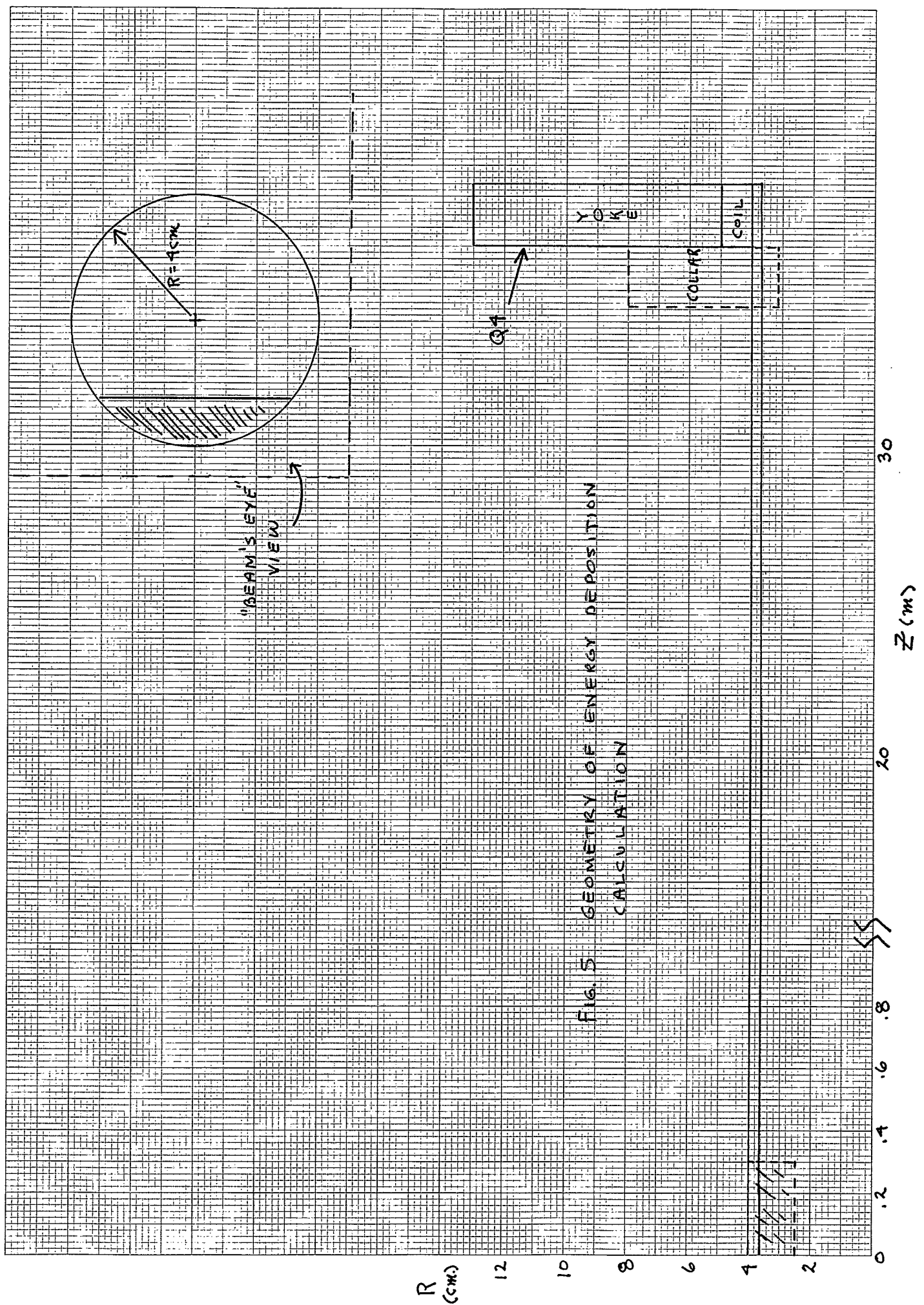


FIG. 5
GEOMETRY FOR ENERGY DEPOSITION

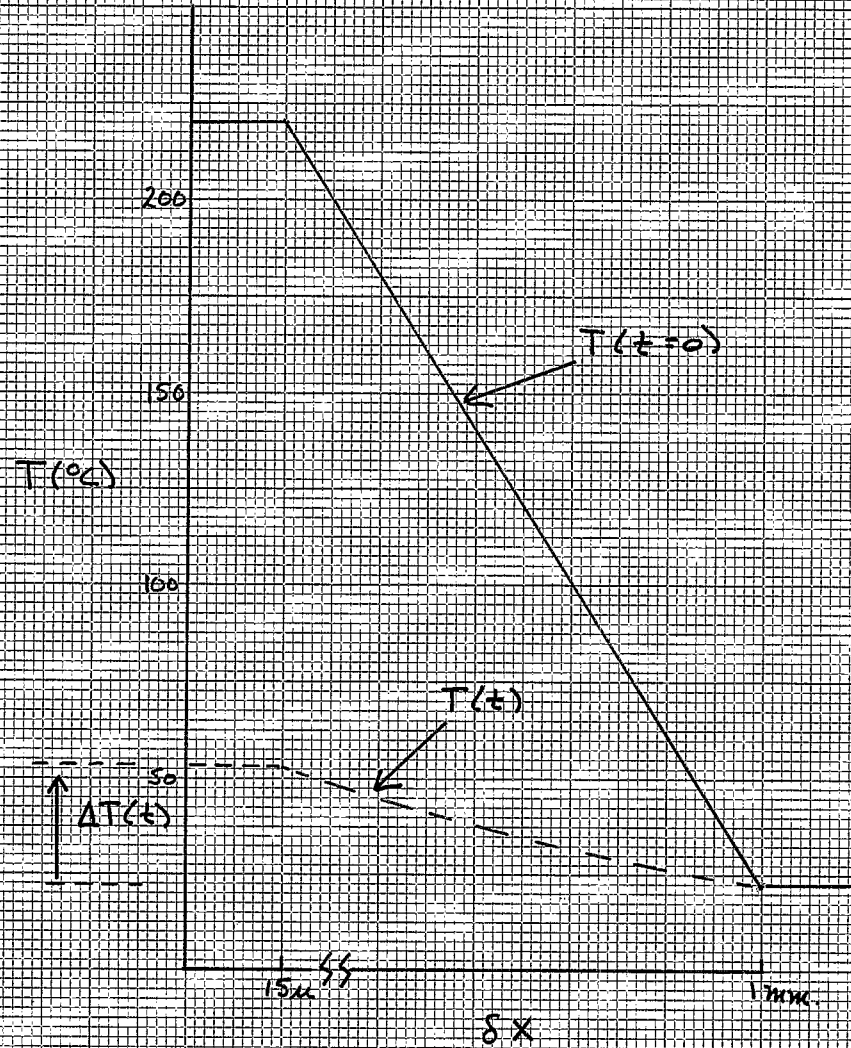


Fig. 6. Illustration of the Transient Heat Transport Calculation used to Estimate Scraper Edge Cooling (see text)